SENSOR AND SIMULATION NOTES

NOTE 196

The Damping of Tank Oscillations with Conducting Dielectric Shells

May 1974

Michael A. Messier
C. L. Longmire
Mission Research Corporation

ABSTRACT

This note is specifically concerned with the electromagnetic properties of the evacuated steel tank used to support the satellite environment in SGEMP simulations. Since the tank is a good conductor it does not allow the radio frequency energy to escape easily. Thus oscillations or ringing modes are set up at discrete frequencies which are executed either by the satellite's EM radiation or by photoelectric currents in tank volume. Methods are examined for keeping the tank model oscillations small so they will not seriously degrade the quality of the simulation. (This note was originally prepared as Tank Physics Memo #7, October 1972).

TABLE OF CONTENTS

LIST OF ILLUSTRATIONS

1. INTRODUCTION

This tank memo is one of a series devoted to the problem of building a simulator which can be used to test a satellite for its vulnerability to the system generated electromagnetic pulse (EMP), i.e., EMP generated by the interaction of photons (primarily x-rays) with the system itself. The best simulation would obviously be the exposure of active systems in orbit to actual nuclear bursts. Since this is not completely practical, we are faced with the problem of reproducing the actual environment as best we can here on terra firma.

This note is specifically concerned with the electromagnetic properties of the evacuated steel tank which is used to support the satellite environment. Being a good conductor, the tank does not allow radio frequency electromagnetic energy to escape easily and hence sets up oscillations or ringing modes at discrete frequencies which are excited either by the satellite's EM radiation or by photoelectric currents in the tank volume. One would like to keep the amplitude of these tank model oscillations small, so that they will not seriously degrade the quality of simulation. It might not be necessary to take any deliberate steps to reduce the ringing, if it occurs after the satellite signal has significantly decreased or if the ringing can be unfolded from the measurements.

If mode damping (Q-spoiling) is required, there are a number of possible methods available, some of which are discussed in this memo. The method chosen depends on several factors, including

(1) the rate of damping required, (2) cost (dollars), (3) cost (working volume sacrificed), and (4) the complexity of the mode excitation. We will investigate two basic methods which seem practical. The first is the use of a thin highly conducting membrane set some distance away from the tank wall. The second is the use of a conducting dielectric layer of some thickness attached to the tank wall. The investigation is primarily limited to layers with constant conductivity, but some variations of conductivity with depth were considered. In practice, both the thin membrane and conducting layer would be modeled by wire grids.

The investigation was based upon planer reflectivity rather than spherical cavity calculations, since one can reasonably relate the cavity Q with the wall reflectivity for a useful class of problems. This approach significantly reduces the complexity of the calculations. The accuracy of these approximations should be adequate for our purposes.

The authors recommend that those readers who are not familiar with the subject of cavity oscillations read Stratton's discussion (Stratton, 1941). The notation used in this memo is Stratton's.

2. THE EFFECT OF IMPERFECTLY CONDUCTING WALLS ON CAVITY RESONANCE MODES

If a cavity with perfectly conducting walls is excited, energy is put into the natural ringing modes. Since no energy can escape, these oscillations at discrete frequencies will continue forever. If the walls have a finite, but large, conductivity, a small amount of energy will be absorbed as joule losses in the wall and the oscillations will slowly decay. The decay is expressed as an imaginary frequency component so that one now speaks of a complex frequency. In addition, the real part of the frequency will shift slightly. It is important to know for what range of wall conductivity, or reflection coefficient, these frequency shifts can be neglected so that the reflection calculations will be valid without correcting the

undamped frequency.

The equations to be solved are derived by Stratton (Stratton, 1941). There are two types of modes: the electric modes and the magnetic modes. The magnetic modes are characterized by a radial magnetic field and no radial electric field. The opposite is true for the electric mode. A net azimuthal current component is required to excite the magnetic mode and, since this seems likely to be less significant than the radial currents in the satellite test configurations, we restrict ourselves to the electric modes.

Consider a sphere of radius a, permittivity ε_1, permeability μ_1, and conductivity σ_1 imbedded in a homogeneous medium characterized by ε_2, μ_2, and σ_2 (rationalized MKSQ units used throughout). The vector wave equation reduces to the following scaler equations for $r < a$ (spherical coordinates, electric mode):

$$E_r^i = - n(n + 1)Y_{mn}^i \frac{j_n(k_1 r)}{k_1 r} e^{i\omega t} \tag{2-1}$$

$$E_\theta^i = - \frac{\partial Y_{mn}^i}{\partial \theta} \frac{1}{k_1 r} [k_1 r j_n(k_1 r)]' e^{i\omega t} \tag{2-2}$$

$$E_\phi^i = - \frac{1}{\sin\theta} \frac{\partial Y_{mn}^i}{\partial \phi} \frac{1}{k_1 r} [k_1 r j_n(k_1 r)]' e^{i\omega t} \tag{2-3}$$

$$H_r^i = 0 \tag{2-4}$$

$$H_\theta^i = - \frac{k_1}{i\omega\mu_1} \frac{1}{\sin\theta} \frac{\partial Y_{mn}^i}{\partial \phi} j_n(k_1 r) e^{i\omega t} \tag{2-5}$$

$$H_\phi^i = \frac{k_1}{i\omega\mu_1} \frac{\partial Y_{mn}^i}{\partial \theta} j_n(k_1 r) e^{i\omega t} . \tag{2-6}$$

For $r > a$,

$$E_r^e = - n(n + 1)Y_{mn}^e \frac{h_n^{(1)}(k_2 r)}{k_2 r} e^{i\omega t} \tag{2-7}$$

$$E_\theta^e = -\frac{\partial Y_{mn}^e}{\partial\theta}\frac{1}{k_2 r}[k_2 r h_n^{(1)}(k_2 r)]' e^{i\omega t} \tag{2-8}$$

$$E_\phi^e = -\frac{1}{\sin\theta}\frac{\partial Y_{mn}^e}{\partial\phi}\frac{1}{k_2 r}[k_2 r h_n^{(1)}(k_2 r)]' e^{i\omega t} \tag{2-9}$$

$$H_r^e = 0 \tag{2-10}$$

$$H_\theta^e = -\frac{k_2}{i\omega\mu_2}\frac{1}{\sin\theta}\frac{\partial Y_{mn}^e}{\partial\phi} h_n^{(1)}(k_2 r) \tag{2-11}$$

$$H_\phi^e = \frac{k_2}{i\omega\mu_2}\frac{\partial Y_{mn}^e}{\partial\theta} h_n^{(1)}(k_2 r) \tag{2-12}$$

where $j_n(\rho)$ and $h_n^{(1)}(\rho)$ are spherical Bessel functions of the first and third kind, respectively and

$$[k_1 r j_n(k_1 r)]' \equiv \frac{\partial}{\partial\rho}[\rho j_n(\rho)]\Big|_{\rho=k_1 r} \tag{2-13}$$

etc. The quantities k_1 and k_2 are the propagation factors in media 1 and 2. The tesseral harmonics are

$$Y_{mn}^i = (B_{emn}^i \cos m\phi + B_{omn}^i \sin m\phi) P_n^m(\cos\theta) \tag{2-14}$$

with i replaced by e in the external media and P_n^m the associated Legendre polynomials. At the surface of the sphere, the continuity of the tangential fields leads to the relation

$$\frac{\mu_1}{k_1^2}\frac{[k_1 a j_n(k_1 a)]'}{j_n(k_1 a)} = \frac{\mu_2}{k_2^2}\frac{[k_2 a h_n^{(1)}(k_2 a)]'}{h_n^{(1)}(k_2 a)} . \tag{2-15}$$

If the external medium is an infinite conductor, the tangential electric field would be zero at r = a ($k_2 = \infty$) and the resonance modes would be determined instead by

$$[k_1 a j_n(k_1 a)]' = 0 . \tag{2-16}$$

If the roots $\rho_{ns} = k_1 a$ of Equation 2-15 are known, the complex resonance frequencies can be found immediately from

$$\rho_{ns}^2 = (k_1 a)^2 = (\omega_{ns}^2 \varepsilon_1 \mu_1 + i\omega_{ns} \mu_1 \sigma_1) a^2 \tag{2-17}$$

or

$$\omega_{ns} = \frac{1}{\varepsilon_1 \mu_1} \left[\sqrt{\frac{\varepsilon_1 \mu_1 \rho_{ns}^2}{a^2} - \frac{\mu_1^2 \sigma_1^2}{4}} - i \frac{\mu_1 \sigma_1}{2} \right]. \tag{2-18}$$

For the special case in which the internal medium is vacuum,

$$\omega_{ns} = \frac{c\rho_{ns}}{a} . \tag{2-19}$$

Define $k_1 a = \rho$, $M = k_1/k_2$, so that Equation 2-15 becomes

$$\frac{[\rho j_n(\rho)]'}{j_n(\rho)} = \frac{\mu_2}{\mu_1} \frac{1}{M^2} \frac{[M\rho h_n^{(1)}(M\rho)]'}{h_n^{(1)}(M\rho)} . \tag{2-20}$$

If the wall is a good conductor, k_2 and M will be large and an asymptotic expansion of $h_n^{(1)}(M\rho)$ can be used. It will be seen that the expansion is rapidly converging so that $M\rho$ does not have to be extremely large for the expansion to be accurate and will be valid for relatively low values of σ_2. We will then assume that the roots do not vary greatly from the roots of Equation 2-16, i.e., from the roots of the infinitely conducting wall problem, and perform a perturbation type calculation.

The function of the third kind can be written as

$$h_n^{(1)}(\rho) = \frac{(-1)^{n+1}}{\rho} e^{i\rho} \left[P_{n+1/2}(\rho) + iQ_{n+1/2}(\rho) \right] \tag{2-21}$$

where

$$P_{n+1/2}(\rho) = 1 - \frac{n(n^2 - 1)(n + 2)}{2^2 \cdot 2!\rho^2} + \frac{n(n^2 - 1)(n^2 - 4)(n^2 - 9)(n + 4)}{2^4 \cdot 4!\rho^4} - \cdots \tag{2-22}$$

$$Q_{n+1/2}(\rho) = \frac{n(n+1)}{2 \cdot 1!\rho} - \frac{n(n^2-1)(n^2-4)(n+3)}{2^3 \cdot 3!\rho^3} + \ldots \qquad (2\text{-}23)$$

It can be seen that these expansions have a finite number of terms for a given n. Choosing the first term in each series,

$$h_n^{(1)}(\rho) \simeq \frac{(-i)^{n+1}}{\rho} e^{i\rho}\left[1 + i\,\frac{n(n+1)}{2\rho}\right]. \qquad (2\text{-}24)$$

For $\rho >> \frac{1}{2} n(n+1)$

$$h_n^{(1)}(\rho) \simeq \frac{(-i)^{n+1}}{\rho} e^{i\rho} \qquad (2\text{-}25)$$

and

$$[\rho h_n^{(1)}(\rho)]' = i\rho h_n^{(1)}(\rho) \; . \qquad (2\text{-}26)$$

Equation 2-20 becomes

$$[\rho j_n(\rho)]' \simeq i\left(\frac{\mu_2}{\mu_1}\right)\left(\frac{\rho}{M}\right) j_n(\rho) \; . \qquad (2\text{-}27)$$

Let ρ_{ns} represent the roots of Equation 2-16, i.e.,

$$[\rho_{ns} j_n(\rho_{ns})]' = 0 \qquad (2\text{-}28)$$

and assume

$$\rho = \rho_{ns} + \Delta\rho_{ns}$$

where $\Delta\rho_{ns} << \rho_{ns}$. Then, using Taylor expansions about ρ_{ns},

$$[\rho_{ns} j_n(\rho_{ns})]'' \Delta\rho \simeq i\,\frac{\mu_2}{\mu_1}\,\frac{\rho_{ns} + \Delta\rho_{ns}}{M} \; .$$

$$[j_n(\rho_{ns}) + j_n'(\rho_{ns})\Delta\rho_{ns}] \; . \qquad (2\text{-}29)$$

The spherical Bessel functions satisfy the radial part of the wave equation

$$r^2 \frac{d^2f}{dr^2} + 2r \frac{df}{dr} + [k^2r^2 - n(n + 1)]f = 0 \tag{2-30}$$

$$r[rf(r)]'' + [k^2r^2 - n(n + 1)]f = 0 \tag{2-31}$$

so that

$$[\rho_{ns} j_n(\rho_{ns})]'' = \frac{j_n(\rho_{ns})}{\rho_{ns}} [\rho_{ns}^2 - n(n + 1)] \tag{2-32}$$

and

$$\Delta\rho_{ns}\left\{[\rho_{ns}^2 - n(n + 1)] - i \frac{\mu_2}{\mu_1} \frac{1}{M} [\rho_{ns} j_n'(\rho_{ns}) + j_n(\rho_{ns})]\right\}$$

$$\simeq - i\left(\frac{\mu_2}{\mu_1}\right)\frac{\rho_{ns}}{M} j_n(\rho_{ns}) . \tag{2-33}$$

Ignoring the second term in brackets because of 1/M,

$$\Delta\rho_{ns} \simeq - i\left(\frac{\mu_2}{\mu_1}\right)\frac{\rho_{ns}}{M} \frac{j_n(\rho_{ns})}{\rho_{ns}^2 - n(n + 1)} . \tag{2-34}$$

In many cases, $\rho_{ns}^2 >> n(n + 1)$ since the smallest ρ_{ns} for each n is greater than n, and Equation 2-34 further reduces to

$$\Delta\rho_{ns} \simeq - i\left(\frac{\mu_2}{\mu_1}\right)\frac{j_n(\rho_{ns})}{\rho_{ns} M} . \tag{2-35}$$

Remembering that $M = k_2/k_1$,

$$\Delta\rho_{ns} \simeq - i \frac{\mu_2}{\mu_1} \frac{\rho_{ns}^2}{k_2 a} \frac{j_n(\rho_{ns})}{\rho_{ns}^2 - n(n + 1)} . \tag{2-36}$$

But, for good conductors,

$$k_2 = (1 + i) \frac{1}{\delta} \tag{2-37}$$

where δ is the skin depth of the material,

$$\delta = \sqrt{\frac{2}{\mu_2 \sigma_2 \omega}} . \tag{2-38}$$

Since ω is assumed to change little and since δ varies only as the square root of ω, one can use

$$\omega = \omega_{ns} = \frac{c\rho_{ns}}{a} . \tag{2-39}$$

Equation 2-36 becomes

$$\Delta\rho_{ns} \simeq - (1 + i) \frac{\mu_2}{\mu_1} \frac{\rho_{ns}^2 \delta}{2a} \frac{j_n'(\rho_{ns})}{\rho_{ns}^2 - n(n + 1)} \tag{2-40}$$

or, for $\rho_{ns}^2 >> n(n + 1)$

$$\Delta\rho_{ns} \simeq - (1 + i) \frac{\mu_2}{\mu_1} \frac{\delta}{2a} j_n'(\rho_{ns}) . \tag{2-41}$$

The change in frequency is given by

$$\Delta\omega_{ns} = \frac{c}{a} (\Delta\rho_{ns}) \equiv - \Delta_{ns}(1 + i) . \tag{2-42}$$

Because the change is complex, there is both a real frequency shift and a damping term.

Table 2-1 lists the ρ_{ns} for several n and s. In order to estimate the importance of the frequency shift, we will calculate $\Delta\rho_{ns}/\rho_{ns}$ for n = s = 1 and several σ_2, assuming a cavity radius of 10 meters. This is a worse case since δ will be smaller for all other ω_{ns} and $j_n'(\rho_{ns})$ does not exceed unity. Using $\rho_{11} = 2.74$, $j_1'(\rho_{11}) = 0.388$ and $\mu_1 = \mu_2 = \mu_0 = 4\pi \times 10^{-7}$ henry/m, we have:

$$\omega_{ns} = 8.22 \times 10^7 \text{ rad/sec}$$

$$f_{ns} = 13.1 \text{ MHz}$$

$$\delta = \frac{0.139}{\sqrt{\sigma}}$$

$$\frac{\Delta\rho_{ns}}{\rho_{ns}} = \frac{\Delta\omega_{ns}}{\omega_{ns}} = - (1 + i)(9.65 \times 10^{-3})\delta .$$

Table 2-1. Roots ($\rho_{ns} = ka$) of mode equation for a cavity with a perfectly conducting wall.

n \ s	1	2	3	4	5
1	2.744	6.117	9.312	12.486	15.644
2	3.870	7.443	10.713	13.921	17.103
3	4.974	8.722	12.064	15.314	18.524
4	6.062	9.968	13.380	16.674	19.916

Table 2-2 shows δ and Δ_{ns}/ω_{ns} for several values of σ ranging from 10^8 mho/m to 1 mho/m. The worst variation for this range is about a tenth of 1 percent. The calculations also show that the wave attenuation is very small. These results are not valid if the wall is not a simple homogeneous medium and the absorption is not that which is due to simple joule losses. It would then be desirable to calculate the complex frequency shift in terms of energy absorption at the wall rather than directly through σ_2. This calculation will not be performed in this memo, but we will generalize the results obtained thus far.

With absorbing walls, the time dependence of the electromagnetic field in the cavity is

$$T(t) = e^{i(\omega_{ns} - \Delta_{ns})t} e^{-\Delta_{ns}t} \tag{2-43}$$

when the absorption is not too great. The frequency shift is the same as the damping constant to a first approximation. Define a quantity Q such that the field amplitude decays as $\exp\left(-\frac{\omega}{2Q}t\right)$ where $\omega = \omega_{ns} - \Delta_{ns}$. Q is discussed in the next section. Then

$$\Delta_{ns} \simeq \frac{\omega_{ns} - \Delta_{ns}}{2Q} \tag{2-44}$$

or

$$\Delta_{ns} \simeq \frac{\omega_{ns}}{2Q + 1} . \tag{2-45}$$

Table 2-2. Skin depths and frequency shifts associated with various conductivity walls for a 10-meter spherical cavity (first electrical mode, E_{11}).

σ_2	δ	Δ_{ns}/ω_{ns}
10^8	1.39E-5	1.34E-7
10^7	4.40E-5	4.25E-7
10^6	1.39E-4	1.34E-6
10^5	4.40E-4	4.25E-6
10^4	1.39E-3	1.34E-5
10^3	4.40E-3	4.25E-5
10^2	1.39E-2	1.34E-4
10	4.40E-2	4.25E-4
1	1.39E-1	1.34E-3

The frequency shift can be related to a measurement of field decay in this manner as long as the Q is such that $\Delta_{ns} << \omega_{ns}$, i.e.,for a relatively high Q. However, for our purposes, the error should be tolerable for the entire range of Q encountered in our calculations.

3. THE RELATIONSHIP BETWEEN CAVITY Q AND WALL REFLECTIVITY

A commonly used measure for the energy containing ability of a cavity is the quality factor Q, defined by

$$Q \equiv \frac{\omega \cdot (\text{energy in cavity})}{(\text{energy dissipated/second})} . \qquad (3\text{-}1)$$

This definition is equivalent to saying that the energy contained in the cavity decays as

$$\mathscr{E} \sim \exp\left(-\frac{\omega}{Q} t\right) \qquad (3\text{-}2)$$

where ω is the frequency of oscillation. Q is properly calculated for a particular tank configuration and oscillation mode by integrating the energy density over the volume and the normal component of the Poynting vector over the surface. It would be simpler to make estimations of the effect of various damping methods if one could relate the reflection properties of a wall material with the Q of a specific cavity/mode configuration. Then one could calculate the reflection properties using plane wave approximations rather than making a calculation for the cavity configuration. This should be possible under the condition that the radial distance to the effective cavity wall is much greater than thickness of the region in which the interaction is taking place. For example, if one is considering simply an imperfectly conducting metal wall, the condition would be that the radius to the wall be much greater than the skin depth of the frequency of interest. This statement is made under the assumption that the damping device does not significantly distort the characteristics of the resonance mode.

Let the average EM energy density in a cavity be $\overline{\mathscr{E}}$. The energy flowing through a square meter in 1 second is

$$\overline{S} = c\overline{\mathscr{E}} \tag{3-3}$$

where c is the speed of light. The energy flow (power) reflection coefficient, R, is defined as the ratio of the reflected energy flow to the incident energy flow. Then, according to Equation 3-1,

$$Q = \frac{\omega \overline{\mathscr{E}} V}{\overline{S}(1 - R)A} \tag{3-4}$$

or

$$Q = \frac{\omega \overline{\mathscr{E}}}{\overline{S}} \frac{g}{1 - R} \tag{3-5}$$

where the geometric factor $g = V/A$ is the ratio of the cavity volume to the effective surface area through which energy is flowing, i.e.,

g is the mean distance traveled by the energy between reflections. Finally, by Equation 3-3 and $k_0 = \omega/c$,

$$Q = \frac{k_0 g}{1 - R} . \tag{3-6}$$

By Equation 5-4 and 5-13, for a highly conducting surface ($k_0\delta \ll 1$)

$$R \simeq \frac{1 - k_0\delta}{1 + k_0\delta}$$

or

$$R \simeq 1 - 2k_0\delta \tag{3-7}$$

where δ is the material's skin depth,

$$\delta = \sqrt{\frac{2}{\mu_0\sigma\omega}} . \tag{3-8}$$

Then, for highly conducting surfaces,

$$Q \simeq \frac{g}{2\delta} . \tag{3-9}$$

We now need to learn how to guess the effective volume-to-surface ratio g, without actually solving the mode problem in detail. In this we may be guided by Q's that have been worked out previously for specific cases. For example, Stratton (1941) gives the formula for a spherical cavity in the lowest electric mode,

$$Q = 0.725 \frac{a}{\delta} . \tag{3-10}$$

Comparing this expression with Equation 3-9, we see that we must have

$$g = 1.45\ a \quad \text{(sphere)} . \tag{3-11}$$

Before interpreting this result, let us examine the simple problem of the mode between two parallel conducting planes a distance D apart, in which the wave vector is purely perpendicular to the planes. Since in this case the energy flow is strictly along the normal direction, it is clear that

$$g = D \quad \text{(planes)} \ . \tag{3-12}$$

Returning now to the sphere, a first inclination might be to replace D by the diameter 2a. However, in the lowest electric mode, the energy does not flow strictly in the radial direction. The distance the energy flows between reflections is more like the mean height of the sphere rather than the mean diameter 2a. The mean height h of a sphere is

$$h = \left(\frac{4\pi}{3} a^3\right) / (\pi a^2) = \frac{4}{3} a \ . \tag{3 13}$$

This suggests that

$$g \simeq h = \frac{4}{3} a \tag{3-14}$$

which indeed is fairly close to Equation 3-11. Note that the correct result indicates a mean distance between reflections a little larger than 4a/3, but a good deal less than 2a.

As long as we are working with spheres, we might as well use Equation 3-11 rather than 3-14.

An interesting thing happens to the value of Q as the reflection coefficient goes to zero; the value of Q has a minimum of

$$Q_{min} = k_0 g \tag{3-15}$$

instead of zero, as one might expect. The finite value follows from the definition of Q and the finite velocity of light which forces the energy to leave a given volume over a finite period of time. For such low values of reflectivity, our approximation (Equation 3-6) for Q is no longer valid. Fortunately, it is the reflectivity, rather than Q, which is of primary interest in discussing the degradation of simulation quality due to the presence of the tank.

4. THE THIN MEMBRANE METHOD

In this section, we calculate the reflection coefficient for a system consisting of a thin conducting membrane in front of a perfectly conducting parallel wall. Figure 4-1 shows the problem geometry. The wall and membrane are in the x-y plane with a plane wave with propagation constant k_0 impinging from the +z direction.

We begin by calculating the amplitude reflection coefficient for the membrane itself. The membrane is required to be of such a conductivity that the thickness of the material is much less than its skin depth while maintaining a finite conductance. Define the dimensionless parameter

$$\beta \equiv Z_0 \sigma d \tag{4-1}$$

as a measure of the conductance, where σ is the membrane conductivity, d is its thickness, and Z_0 is the impedance of free space (120 π ohms). The skin depth is given by

$$\delta = \sqrt{\frac{2}{\mu\omega\sigma}} \tag{4-2}$$

where μ is the permeability of the medium and ω is the signal frequency. The condition

$$d/\delta << 1 \tag{4-3}$$

thus leads to

$$kd << 2/\beta \tag{4-4}$$

and

$$\sigma = \beta/Z_0 d \ . \tag{4-5}$$

For an arbitrary β and $\mu = \mu_0 = 4\pi \times 10^{-7}$ henry/m, Maxwell's equations are

$$\nabla \times \vec{E} = - \dot{\vec{B}} \tag{4-6}$$

$$\nabla \times \vec{H} = \vec{J} + \dot{\vec{D}} \tag{4-7}$$

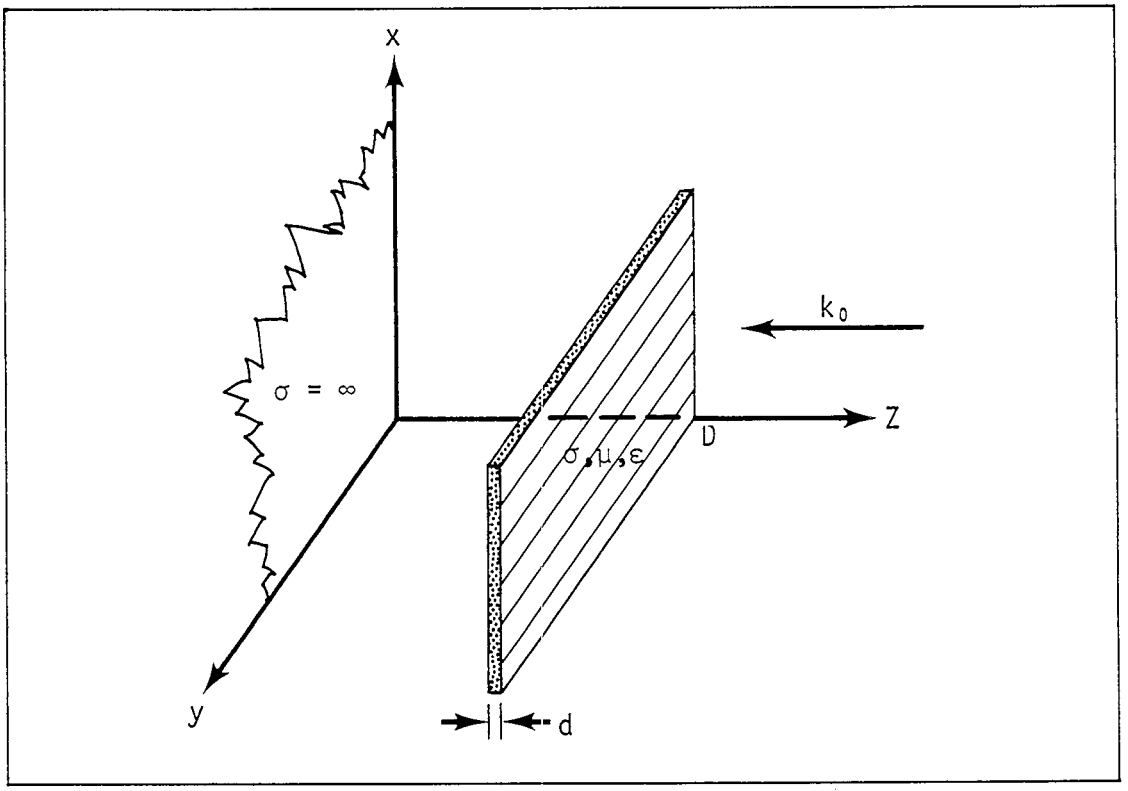

Figure 4-1. Coordinate system for membrane calculation.

where $\mu\vec{H} = \vec{B}$ and $\varepsilon\vec{E} = \vec{D}$. Assuming that the time dependence of the fields is $e^{i\omega t}$,

$$\frac{\partial E_x}{\partial z} = - i\omega B_y \tag{4-8}$$

$$\frac{\partial B_y}{\partial z} = \mu\sigma E_x + i\mu\varepsilon\omega E_x \ . \tag{4-9}$$

Assuming E_x to be constant across the membrane, the integration of Equation 4-9 yields

$$- (B_2 - B_1) = \mu\sigma d E_x \tag{4-10}$$

since we shall choose $\sigma >> \varepsilon\omega$.

The incident, reflected, and transmitted electric fields are related through

$$E_i + E_r = E_t \tag{4-11}$$

and hence, the transmission and reflection coefficients are related by

$$1 + r = t \tag{4-12}$$

where we have defined $E_r \equiv rE_i$ and $E_t \equiv tE_i$. By Equation 4-10, assuming $\mu = \mu_0$,

$$B_i + B_r - B_t = \mu_0\sigma d E_t \ . \tag{4-13}$$

In free space, $E = Bc$ and considering that the reflected B must change sign,

$$1 - r - t = \beta t \tag{4-14}$$

where

$$\beta \equiv \mu_0 c\sigma d = Z_0\sigma d \ . \tag{4-15}$$

Combining Equations 4-12 and 4-14, we find

$$1 + \beta = \frac{1 - r}{1 + r} \tag{4-16}$$

or

$$r = -\frac{\beta}{2 + \beta} . \tag{4-17}$$

Note that r, the amplitude reflection coefficient of the membrane alone, is independent of frequency and depends only upon σd through β.

We now calculate the reflection coefficient of the system composed of the membrane with reflection coefficient r placed a distance D in front of a perfectly conducting wall. A plane wave with propagation constant $k_0 = \omega/c$ is incident upon the system. Let r_s be the amplitude reflection coefficient of the system. Then, with $x = k_0 D$,

$$r_s = r + t^2[\underbrace{-1 \cdot e^{2ix}}_{\substack{\text{one} \\ \text{reflection}}} + \underbrace{(-1)^2 r e^{4ix}}_{\substack{\text{two} \\ \text{reflections}}} + \underbrace{(-1)^3 r^2 e^{6ix}}_{\substack{\text{three} \\ \text{reflections}}} + \ldots] \tag{4-18}$$

or

$$r_s = r - (1 + r)^2 e^{2ix}[1 - re^{2ix} + r^2 e^{4ix} - r^3 e^{6ix} + \ldots] \tag{4-19}$$

which reduces to

$$r_s = r - \frac{(1 + r)^2 e^{2ix}}{1 + re^{2ix}} \tag{4-20}$$

or

$$r_s = \frac{r - (1 + 2r)e^{2ix}}{1 + r^{2ix}} . \tag{4-21}$$

For undamped waves, x is real.

The energy flow reflection coefficient is given by

$$R = |r_s|^2 = \frac{r^2 + (1 + 2r)^2 - 2r(1 + 2r)\cos(2x)}{1 + r^2 + 2r\cos(2x)} . \tag{4-22}$$

R is plotted in Figure 4-2 as a function of $k_0 D/\pi$ for discrete values of r (labeled by absolute value). The curves are symmetric about

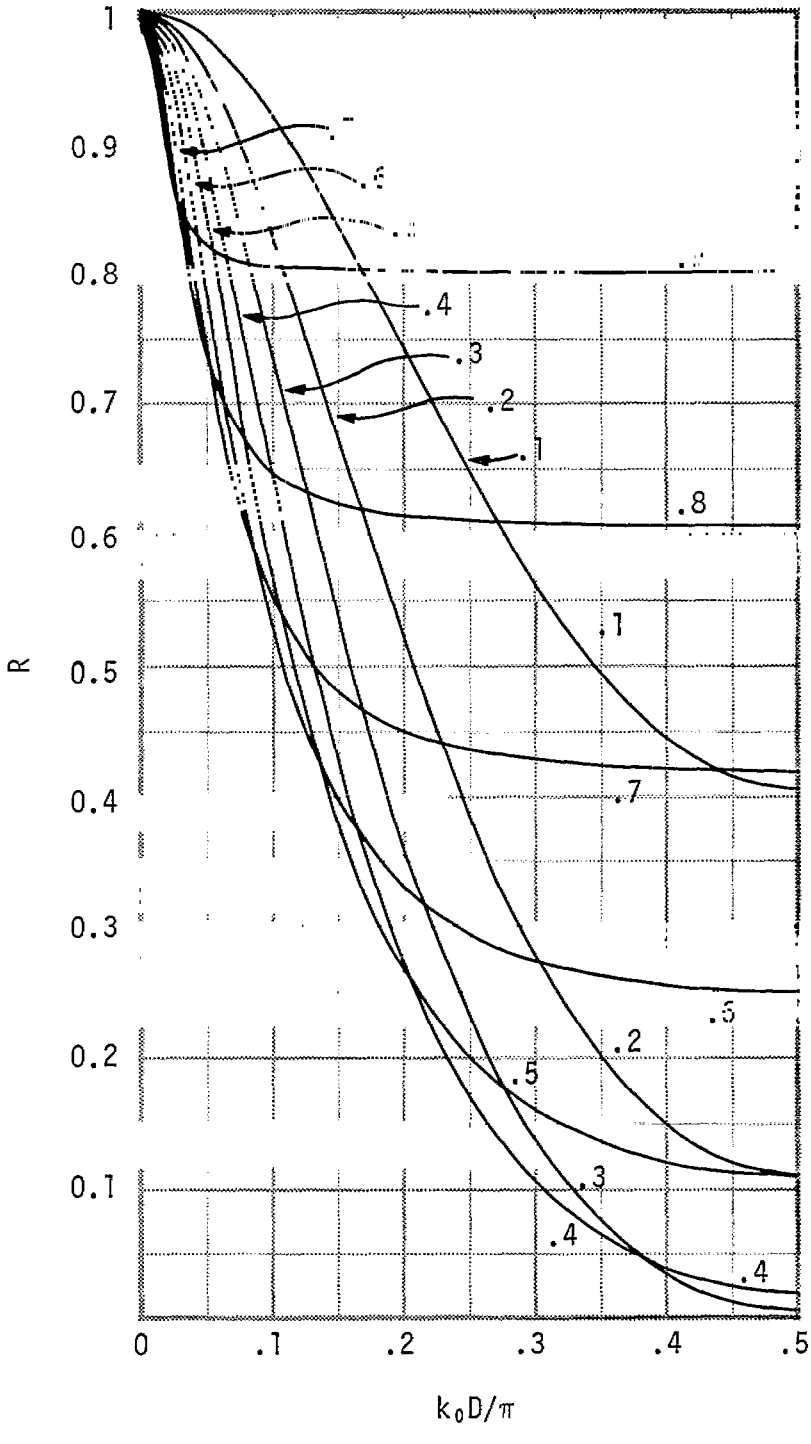

Figure 4-2. Energy flow reflection coefficient vs k_0D/π for various membrane reflectivities.

$k_0D = \pi/2$. Figure 4-3 shows R as a function of k_0D and R for the smaller values of k_0D.

We now illustrate the use of these curves. For the lowest tank mode $k_0R = 2.74$. If we choose the spacing D = 0.2R, leaving 80 percent of the tank radius free, we have $k_0D = 0.549$ then $k_0D/\pi = 0.175$. Figure 4-2 shows that the power reflectivity will be R = 0.31 if we choose the membrane reflectivity -r = 0.5. This should be adequate for this mode since it is not excited very strongly anyway.

Now consider the higher tank modes and the high-frequency satellite modes. The reflectivity will be low for these modes unless one or more of them happens to have a k_0 such that $k_0D \approx n\pi$, where n is an integer. To guard against this possibility one could, given prior knowledge of the modes, choose D so as to avoid it; this would not appear to be a satisfactory method. Alternatively, one could avoid having the membrane lie at constant radius, independent of angle, or one could use two membranes at non-rational distances from the wall. We shall analyze these possibilities further, but believe they would work satisfactorily. A continuous absorbing medium is studied in the following section.

Note that to get -r = 0.5 we need $\beta = 2$. Thus according to Equation 4-15 we need

$$\sigma d = \beta/\mu c = \beta/(377\Omega) = 0.0053 \text{ mhos} . \qquad (4\text{-}23)$$

Then to satisfy the small skin depth condition 4-4, we need

$$d \ll \frac{2}{\beta k_0} = \frac{1}{k_0} \qquad (4\text{-}24)$$

for the highest k_0 considered. If the highest k_0 10 m^{-1} (λ = 0.6 m), this becomes

$$d \ll 0.1 \text{ m} . \qquad (4\text{-}25)$$

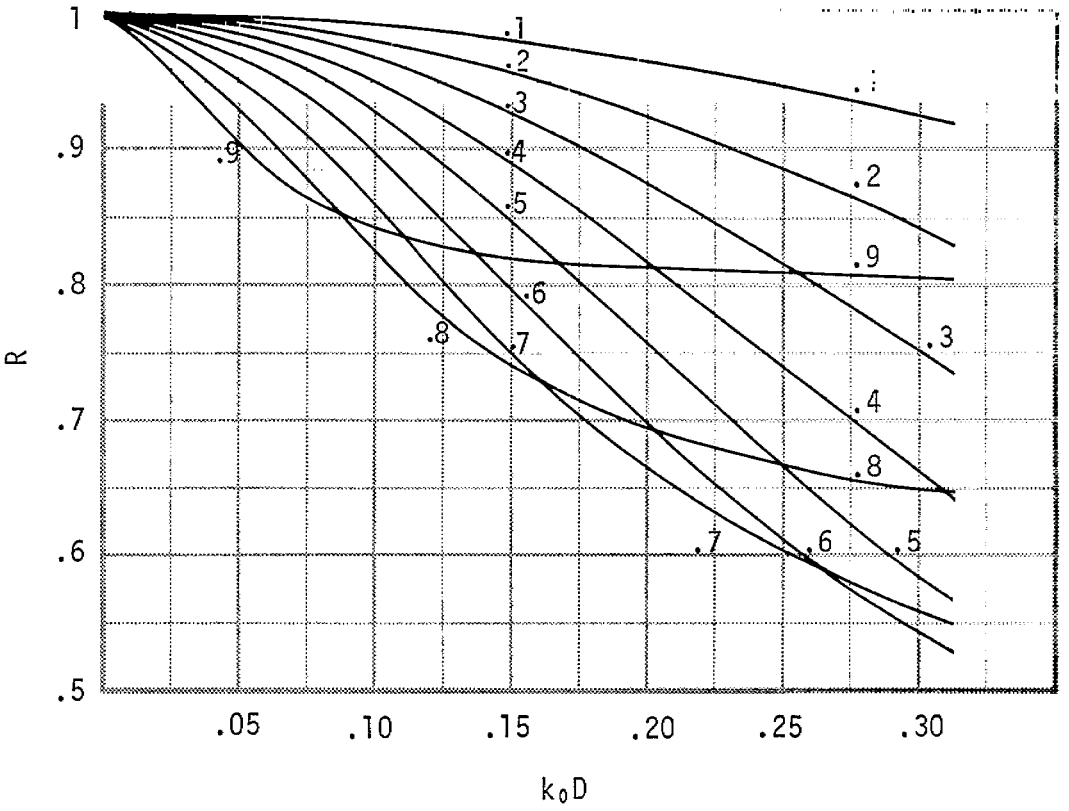

Figure 4-3. Energy flow reflection coefficient vs k_0D for various membrane reflectivities.

We could choose $d = 10^{-3}$ meters, and then find

$$\sigma = \frac{\beta}{Z_0 d} = 5.3 \text{ mho/m} . \qquad (4\text{-}26)$$

In practice one would not use a sheet membrane, because of vacuum and x-ray problems, but would mock it up by a grid of wires having the same impedance per square.

5. THE CONDUCTING DIELECTRIC LAYER METHOD

In this section, we calculate the energy flow reflection coefficient for a conducting dielectric slab in contact with a perfectly conducting wall. The majority of the investigation was for the case where the material properties were uniform throughout the slab thickness. Some time was spent to see if much could be gained by varying the conductivity as a function of depth and a computer code was written which provides the reflection coefficient for an arbitrary one-dimensional variation of σ and ε.

Intuitively, one might doubt that a dielectric layer over the cavity wall could be useful in spoiling the Q of that cavity because one would expect thicknesses on the order of a wavelength to be required, and that is on the order of the cavity diameter for the primary resonant mode. This would be true if wave interference was to be the mechanism for mode attenuation. However, it will be shown that by using a conducting dielectric layer, the cavity Q can be reduced from on the order of a thousand to near unity without losing more than a few percent of the cavity radius. It is likely that greater attenuations can be obtained by giving the layer's conductivity a radial dependence. The feasibility of this basic approach rests with the determination of how much cavity radius can be sacrificed for a desired amount of Q reduction and with the availability of suitable materials.

Stratton has calculated the reflection coefficient of a plane sheet at normal incidence (Stratton, 1941). Let the medium containing the incident wave be medium 1 (see Figure 5-1), let the sheet be medium 2, and let the transmitting medium be medium 3. All are homogeneous and characterized by propagation factors k_1, k_2, k_3, respectively. The energy flow reflection coefficient is given by

$$R = \frac{R_{12} + 2\sqrt{R_{12}R_{23}}e^{-2\beta_2 d}\cos(\delta_{23} - \delta_{12} + 2\alpha_2 d) + R_{23}e^{-4\beta_2 d}}{1 + 2\sqrt{R_{12}R_{23}}e^{-2\beta_2 d}\cos(\delta_{23} + \delta_{12} + 2\alpha_2 d) + R_{12}R_{23}e^{-4\beta_2 d}} \qquad (5\text{-}1)$$

where

R_{jk} = reflection coefficient for a wave in medium j incident upon medium k

$$\tan\delta_{jk} = \frac{2\mu_j\mu_k(\alpha_k\beta_j - \alpha_j\beta_k)}{\mu_k^2(\alpha_j^2 + \beta_j^2) - \mu_j^2(\alpha_k^2 + \beta_k^2)} \qquad (5\text{-}2)$$

δ_{jk} = phase change involved in reflecting from medium k

$\alpha_j = \mathrm{Re}k_j$

$\beta_j = \mathrm{Im}k_j$

d = thickness of medium 2

μ_j = permeability of medium j

For the case of medium 3 being perfectly conducting, $R_{23} = 1$ and $\delta_{23} = 0$. Now, for medium 1 a perfect dielectric and medium 2 a conducting dielectric, we have $\beta_1 = 0$ and (Stratton, 1941)

$$R_{12} = \frac{(\mu_1\alpha_2 - \mu_2\alpha_1)^2 + \mu_1^2\beta_2^2}{(\mu_1\alpha_2 + \mu_2\alpha_1)^2 + \mu_1^2\beta_2^2} . \qquad (5\text{-}3)$$

Assume $\mu_1 = \mu_2 = \mu_0 = 4\pi \times 10^{-7}$ henry/m, and assume medium 1 is free space, so that $\alpha_1 = k_0 = \omega/c$ (where c is the speed of light). Then

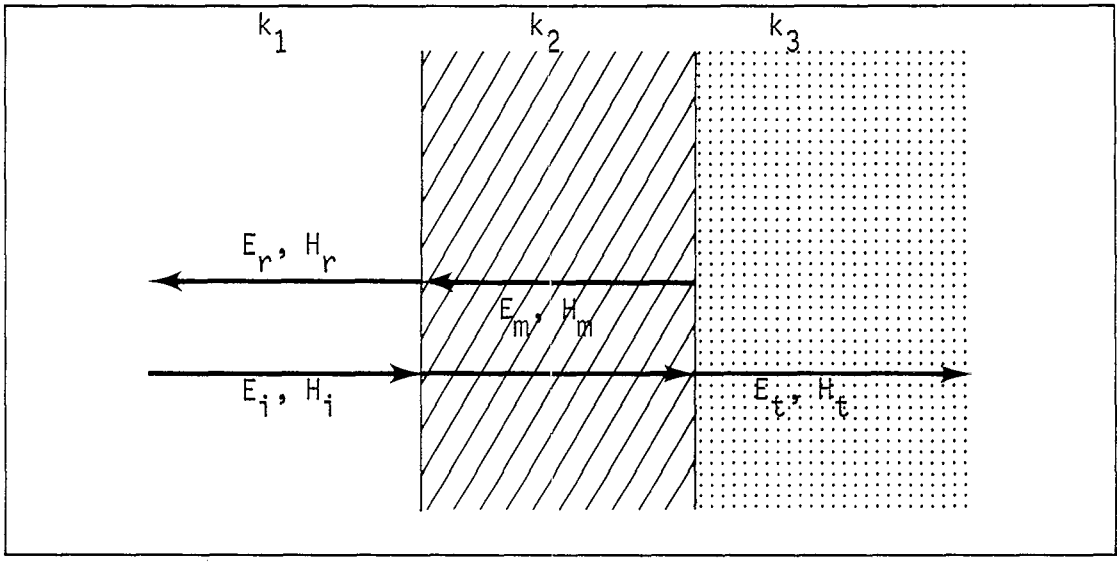

Figure 5-1. Reflection and transmission of plane waves by a plane sheet at normal incidence.

$$R_{12} = \frac{(\alpha_2 - k_0)^2 + \beta_2^2}{(\alpha_2 + k_0)^2 + \beta_2^2} \tag{5-4}$$

and

$$\tan\delta_{12} = \frac{-2k_0\beta_2}{k_0^2 - \alpha_2^2 - \beta_2^2} \, . \tag{5-5}$$

The reflection coefficient becomes

$$R = \frac{R_{12} + 2\sqrt{R_{12}}e^{-2\beta_2 d}\cos(2\alpha_2 d - \delta_{12}) + e^{-4\beta_2 d}}{1 + 2\sqrt{R_{12}}e^{-2\beta_2 d}\cos(2\alpha_2 d + \delta_{12}) + R_{12}e^{-4\beta_2 d}} \, . \tag{5-6}$$

In medium 2, the wave number is

$$k_2 = \omega\sqrt{\varepsilon\mu_0[1 - i(\sigma/\varepsilon\omega)]} \, . \tag{5-7}$$

Let ε_r be the dielectric constant, i.e.,

$$\varepsilon = \varepsilon_r\varepsilon_0 \tag{5-8}$$

so that

$$k_2 = \sqrt{\varepsilon_r}\, k_0\sqrt{1 - i\left(\frac{\sigma}{\varepsilon\omega}\right)} \, . \tag{5-9}$$

Define $k_2 = \alpha_2 + i\beta_2$. Then

$$\alpha_2 = k_0\sqrt{\frac{\varepsilon_r}{2}}\left[\sqrt{1 + \left(\frac{\sigma}{\varepsilon\omega}\right)^2} + 1\right]^{1/2} \tag{5-10}$$

$$|\beta_2| = \frac{1}{2\alpha} k_0^2 \left(\frac{\sigma}{\varepsilon\omega}\right) \tag{5-11}$$

$$\beta_2 = k_0\sqrt{\frac{\varepsilon_r}{2}}\left[\sqrt{1 + \left(\frac{\sigma}{\varepsilon\omega}\right)^2} - 1\right]^{1/2} \tag{5-12}$$

where the positive values have been chosen.

For a good conductor, i.e., $\left(\frac{\sigma}{\varepsilon\omega}\right) >> 1$, these equations reduce to

$$\alpha \simeq \beta \simeq \sqrt{\frac{\omega\mu_0\sigma}{2}} = 1/\delta \tag{5-13}$$

and for a poor conductor, i.e., $(\delta/\varepsilon\omega) << 1$, they reduce to

$$\alpha \simeq \sqrt{\varepsilon_r}k_0\left[1 + \frac{1}{8}\left(\frac{\sigma}{\varepsilon\omega}\right)^2\right] \simeq \sqrt{\varepsilon_r}k_0 \tag{5-14}$$

$$\beta \simeq \frac{k_0}{2\sqrt{\varepsilon_r}}\left(\frac{\sigma}{\varepsilon_0\omega}\right) = \frac{\sigma}{2\sqrt{\varepsilon_r}}Z_0 \tag{5-15}$$

where Z_0 is the impedance of free space (120π ohms).

The study of the energy reflection coefficient (R) of a constant slab was made in two parts. In the first part, the reflecting frequency was considered constant and R was calculated as a function of slab parameters related to thickness and conductivity. In the second part of the study, the slab parameters were initially fixed for the fundamental electric mode and R was studied as a function of frequency.

The studies were performed by numerically calculating Equations 5-4, 5-5, 5-6, 5-8, and 5-9. In the first part, the independent parameters chosen were: k_0d, ε_r, and $(\sigma/\varepsilon\omega)$. From these, all factors required by the equations can be calculated. They have the advantage of not requiring any information about the cavity size. As will be seen, reflectivity minima occur for large values of $(\sigma/\varepsilon\omega)$, i.e., for good conductors. A more useful parameter than $(\sigma/\varepsilon\omega)$ would have been d/δ, where δ is the skin depth. d/δ can be calculated directly from k_0d, ε_r, and $(\sigma/\varepsilon\omega)$:

$$\delta = \sqrt{\frac{2}{\mu\sigma\omega}} = \frac{1}{k_0}\frac{\sqrt{\sigma/\varepsilon\omega}}{\sqrt{2/\varepsilon_r}} \tag{5-16}$$

$$\frac{d}{\delta} = (k_0d)\sqrt{\frac{\varepsilon_r}{2}}\sqrt{\frac{\sigma}{\varepsilon\omega}}\ . \tag{5-17}$$

The three independent variables would then be: $k_0 d$, d/δ, and ε_r.

Figure 5-2 shows R as a function of $(\sigma/\varepsilon\omega)$ for $k_0 d = 0.1$ and 0.2, and for $\varepsilon_r = 1$, 2, and 3. For thicknesses which are a small fraction of the cavity radius, a, the variation in $k_0 d$ can be interpreted simply as a variation in d. Then, by Figure 5-2, if one allows a larger thickness for the dielectric layer, one can achieve a lower reflectivity with a lower conducting material. The minima at constant $k_0 d$ have magnitudes which are nearly independent of ε_r, for ε_r on the order of unity so that there is no advantage to using a material with ε_r other than unity. The points at which $d/\delta = 1$ are indicated by x's on Figure 5-2. The minima occur between $d/\delta = 1.1$ and $d/\delta = 1.2$ and are not much different than the value of R at $d/\delta = 1$. The minima occur at approximately the same value d/δ independently of ε_r. If d/δ is considered constant, then by Equation 5-17, the value of $(\sigma/\varepsilon\omega)$ at R_{min} will be inversely proportional to ε_r and inversely proportional to the square of $k_0 d$. This is indicated by the curves.

In order to make a judgement as to the maximum allowable value of $k_0 d$, one must relate this quantity to the fraction of tank radius implied, i.e.,

$$\frac{d}{a} = \frac{k_0 d}{k_0 a} \tag{5-18}$$

or

$$\frac{d}{a} = \frac{k_0 d}{\rho_{ns}} \tag{5-19}$$

where ρ_{ns} are the roots of the mode equation (see Section 2). For the fundamental electric mode,

$$\rho_{10} = 2.744 \tag{5-20}$$

by Table 2-1, so that for this mode

$$\frac{d}{a} = \frac{k_0 d}{2.744} \, . \tag{5-21}$$

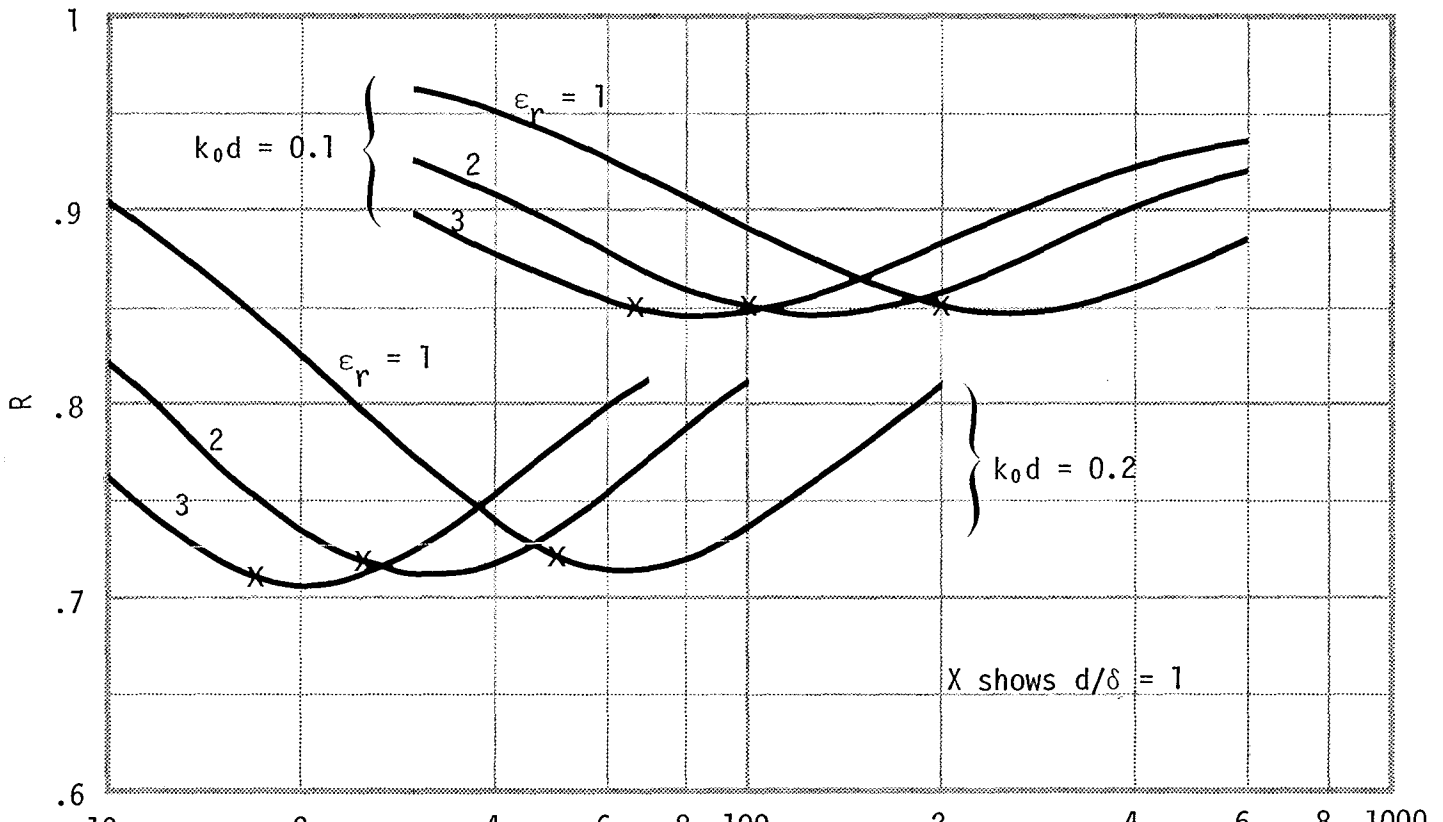

Figure 5-2. Reflection coefficient vs $(\sigma/\varepsilon\omega)$ for various ε_r and k_0d.

Figure 5-3 shows the relationship between d/a and $k_0 d$ for this mode.

The first part of this study was performed for values of $k_0 d$ less than 0.3, corresponding to slab thicknesses of about 10 percent of the tank radius. Later, it was decided that a 20 percent thickness could be tolerated, with corresponding decreases in R, so that values up to $k_0 d = 0.6$ were used. The first part of the study did not need repeating because the lessons learned from it could simply be extrapolated.

The variation of R with $k_0 d$ is shown in Figure 5-4 for $(\sigma/\varepsilon\omega) = 100$ and $\varepsilon_r = 1, 2, 3$. Initially, R decreases with increasing $k_0 d$ due to absorption in the medium and probably some phase effects. A minimum occurs at a value of $k_0 d$ corresponding to $d/\delta \simeq \pi/2$. Larger values of $k_0 d$ produce increasing values of R which asymptotically approach R_{12} after a slight peak. The fact that the minimum in the R - $(\sigma/\varepsilon\omega)$ plane occurs for a different value of d/δ than the minimum in the R - $(k_0 d)$ plane means that there can be no absolute minima in the R - $(k_0 d)$ - $(\delta/\varepsilon\omega)$ surface. This is because two values of d/δ cannot be produced by the same $k_0 d$ - $(\sigma/\varepsilon\omega)$ pair. The surface generated resembles a ravine running down the side of a mountain. At any altitude one can find a local minimum, i.e., the bottom of the ravine. However, one can always find a lower surface level by simply moving down the mountain (increasing $k_0 d$). This is nicely illustrated in Figure 5-5, which shows R vs $(\sigma/\varepsilon\omega)$ for various values of $k_0 d$ and $\varepsilon_r = 1$.

Figure 5-6 shows R vs $k_0 d$ for various values of $(\delta/\varepsilon\omega)$ and $\varepsilon_r = 1$. The curves represent slices through the mountain. The values $(\sigma/\varepsilon\omega) = 65$ and 240 correspond to the local minima at $k_0 d = 0.2$ and 0.1, respectively. Figure 5-7 shows the minimum R as a function of $k_0 d$. The values of R_{min} for $0.2 < k_0 d \leq 0.6$ were taken from the second part of this study. The dashed line is a "guesstrapolation" based on the smooth behavior of the curve.

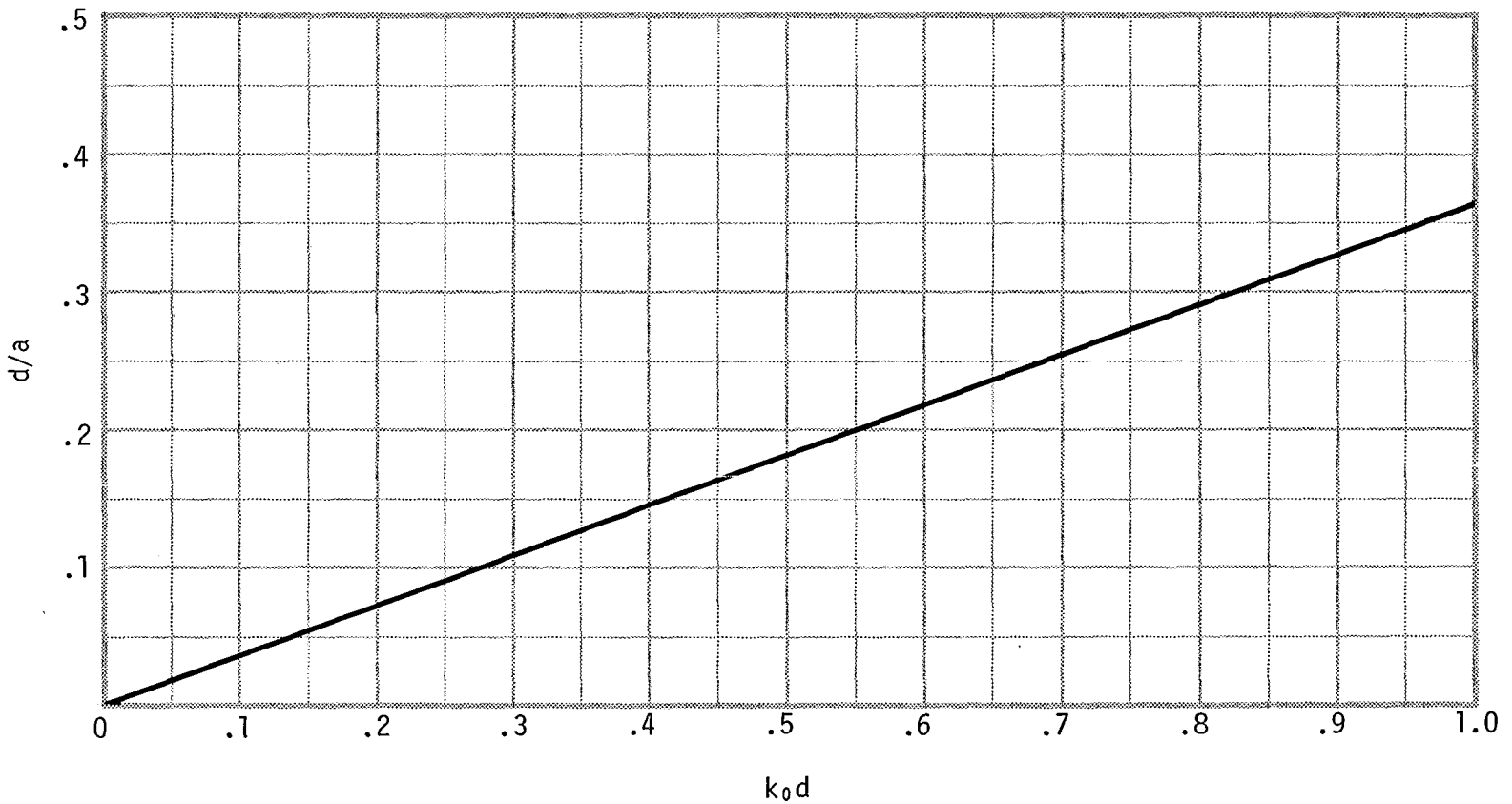

Figure 5-3. Ratio of slab thickness to tank radius as a function of k_0d for the primary electric mode.

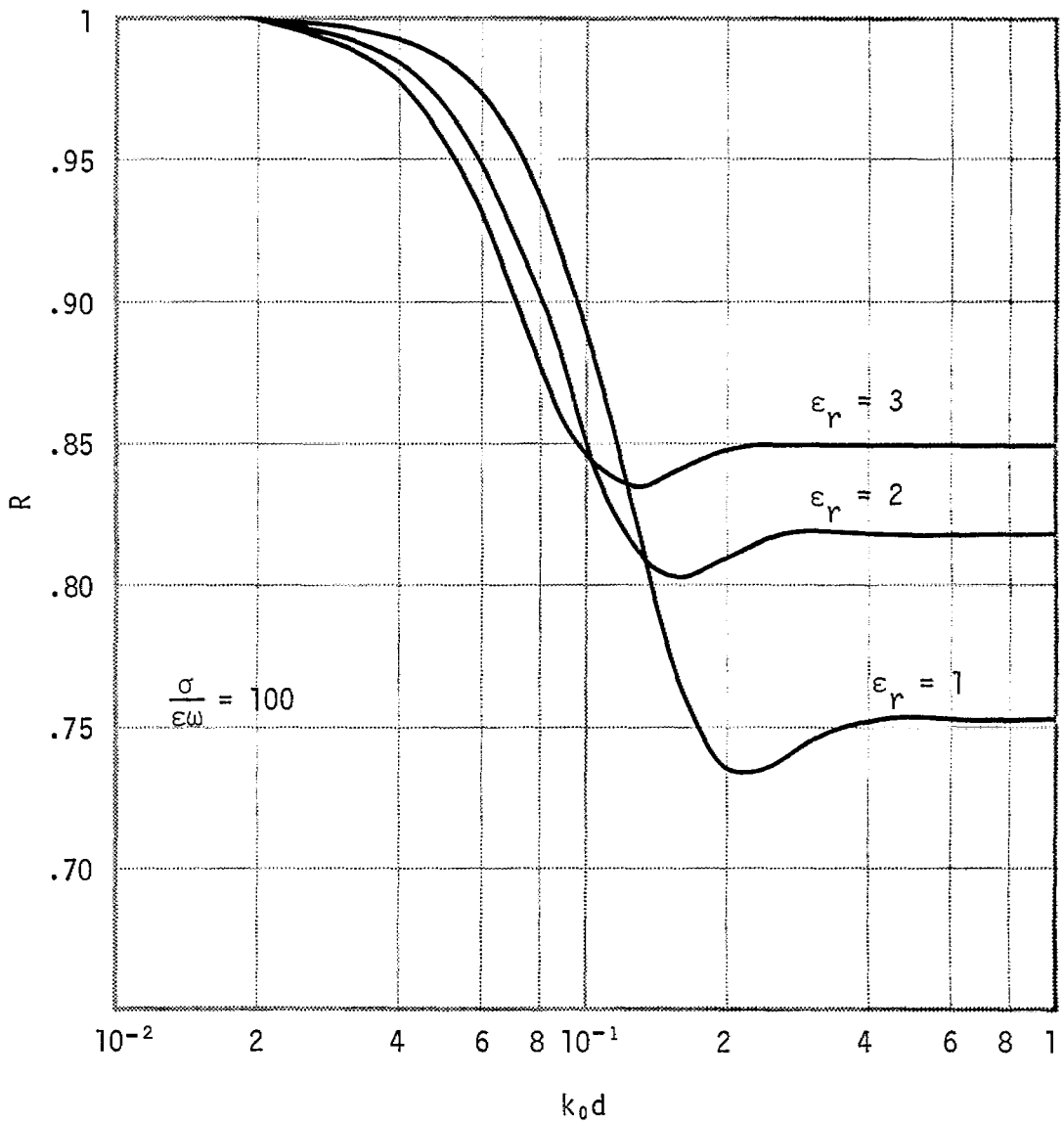

Figure 5-4. Reflection coefficient vs $k_0 d$ for various ε_r.

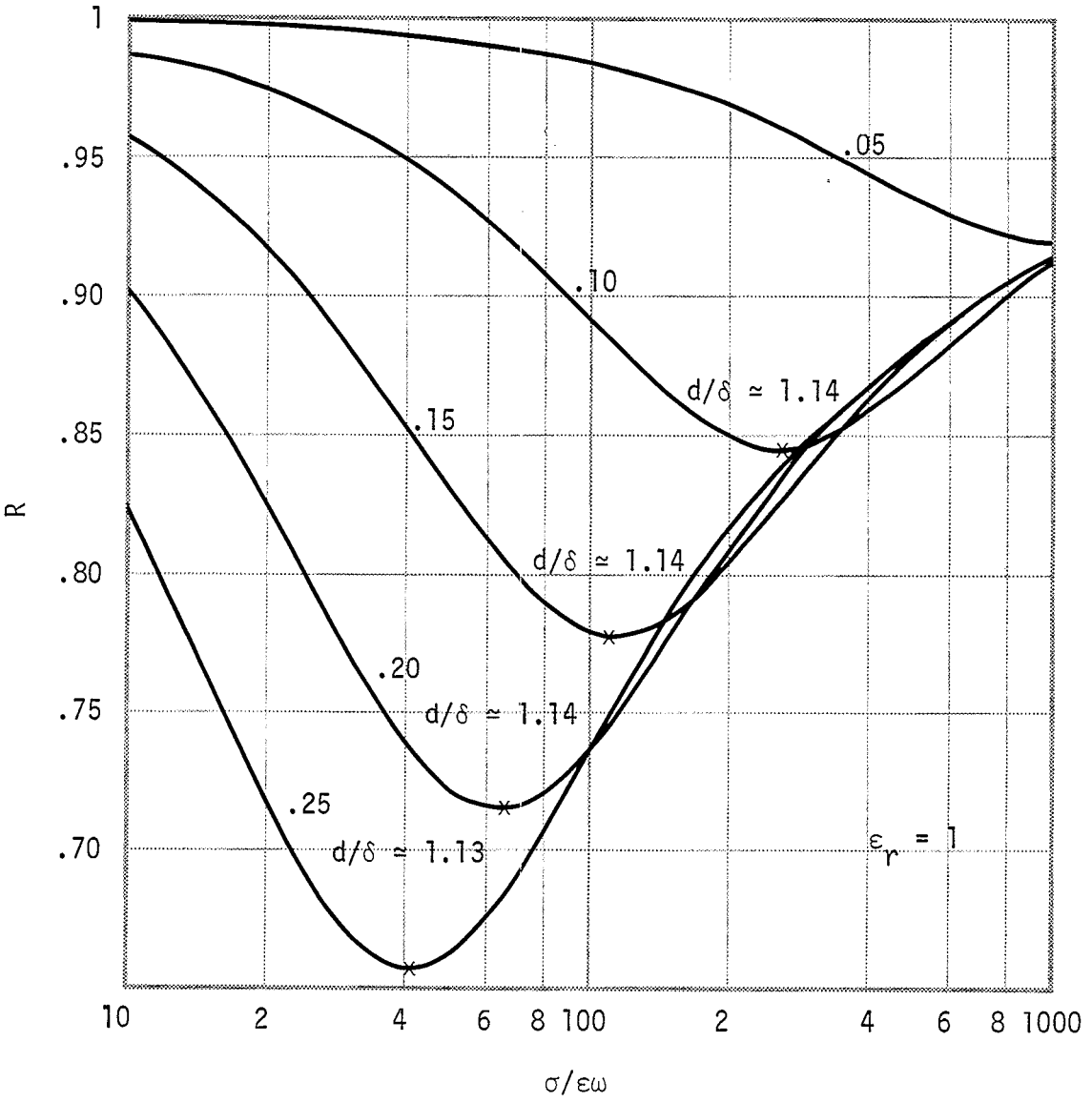

Figure 5-5. Reflection coefficient vs $\sigma/\varepsilon\omega$ for various $k_0 d$.

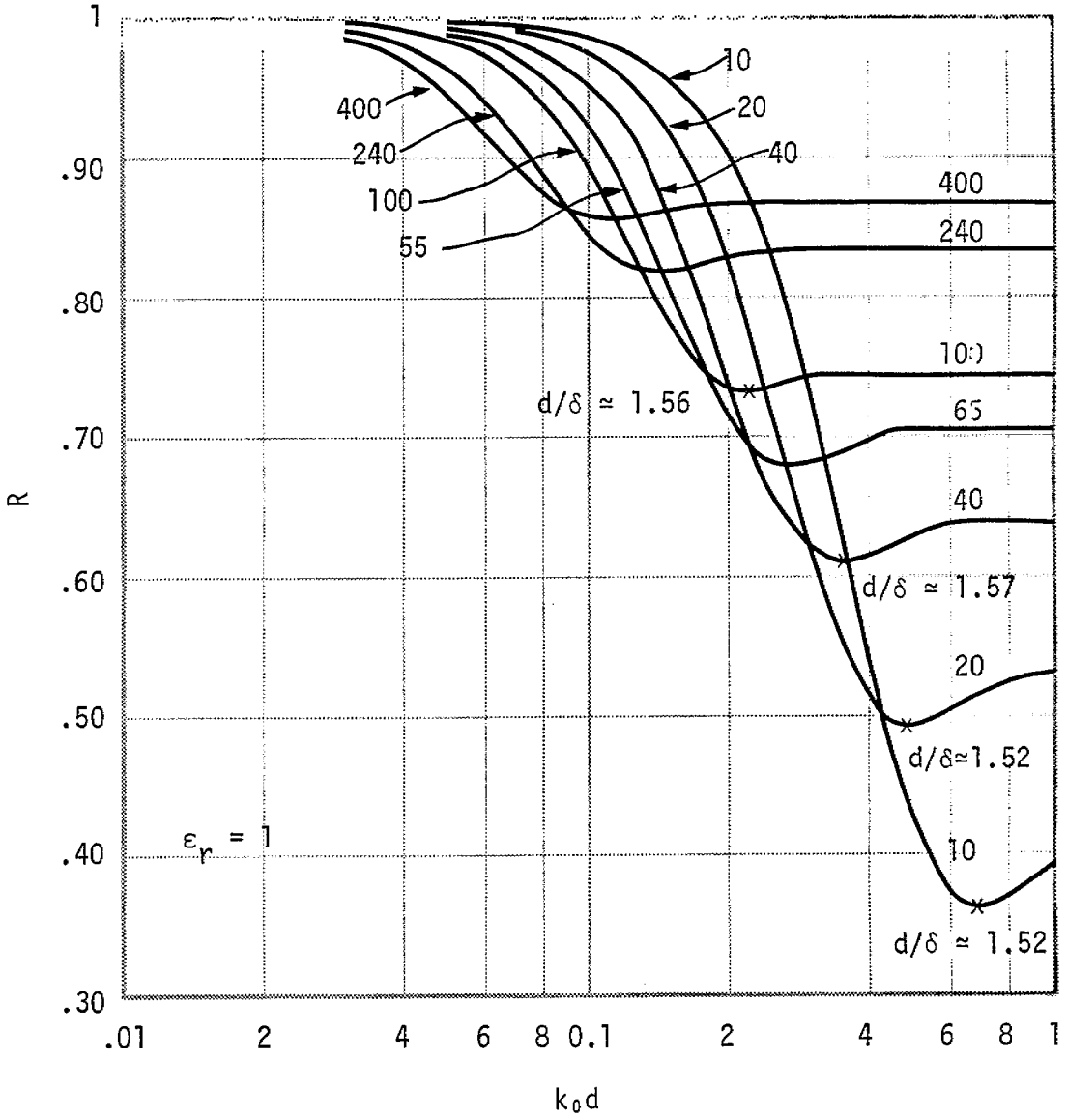

Figure 5-6. Reflection coefficient vs k_0d for various $\sigma/\varepsilon\omega$.

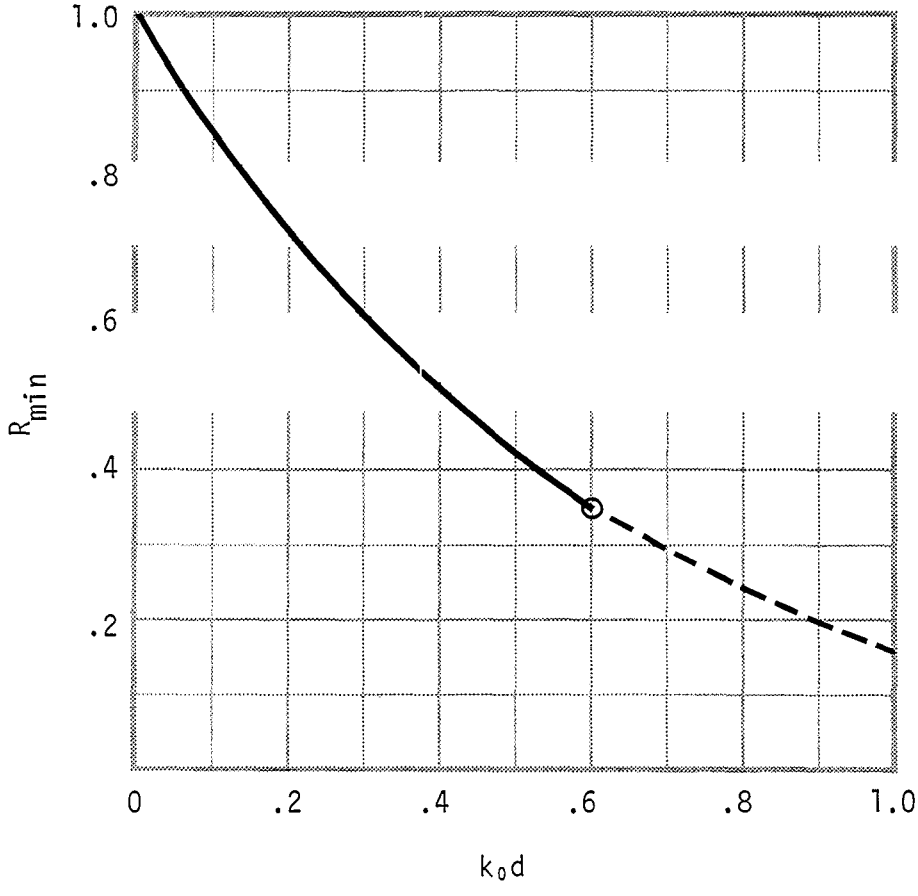

Figure 5-7. Minimum reflection coefficient vs k_0d.

The first part of this study shows that the lowest reflection coefficient, for a given $k_0 d$, is obtained when the material conductivity is such that d/δ is slightly greater than unity (assuming $\varepsilon_r = 1$). Assume that one has established the slab parameters to give a certain R for the fundamental mode. The next question is how does R vary for the higher frequencies. It would be undesirable to have R increase. The answer to this question was the objective of the second part of the study. Table 5-1, based on Table 2-1, shows the tank electric mode frequencies as multiples of the fundamental electric mode frequencies for a few n and s. The frequencies radiated by the satellite itself are different and possibly much higher.

Table 5-1. Tank electric mode frequencies as multiples of the fundamental electric mode frequency.

n \ s	1	2	3	4	5
1	1	2.229	3.394	4.550	5.701
2	1.410	2.712	3.904	5.073	6.233
3	1.813	3.179	4.397	5.581	6.751
4	2.209	3.633	4.876	6.077	7.258

To begin the calculation, one knows that the desirable ratios d/δ are in the range $1 \leq d/\delta < 2$. Desirable values of $k_0 d$ are in the range $0.4 < k_0 d < 0.6$ (a slab thickness which is 20 percent of the tank radius corresponds to $k_0 d = 0.549$). From the definition of skin depth (Equation 5.16) one can calculate the product of the conductivity and thickness as

$$\sigma d = \frac{2}{Z_0 (k_0 d)} (d/\delta)^2 \qquad (5\text{-}22)$$

or the dimensionless parameter

$$\beta = Z_0 (\sigma d) = \frac{2}{k_0 d} (d/\delta)^2 \qquad (5\text{-}23)$$

where Z_0 is the impedance of free space (120π ohms). For a given value of kd, the ratio $(\sigma/\varepsilon\omega)$ can be calculated from

$$(\sigma/\varepsilon\omega) = \beta/kd \tag{5-24}$$

where $k = \omega/c$. One then has the parameters used in the first part of the study for the calculation of R, except that k_0d is replaced by kd. The parameter k_0d now will be used strictly to refer to the fundamental frequency. Since only frequencies higher than the fundamental mode frequency are interesting, the parameter kd was actually replaced by the ratio of frequency to fundamental frequency, i.e.,

$$\frac{\omega}{\omega_0} = \frac{kd}{k_0d} \tag{5-25}$$

where ω_0 is the fundamental frequency.

Figure 5-8 shows R as a function of ω/ω_0 for $d/\delta = 1$ and three values of k_0d (0.6, 0.5, and 0.4). Figure 5-9 shows the same for $d/\delta = 1.2$. The range of ω/ω_0 is from one to one hundred. Except for some inflections and oscillations at higher frequencies, R decreases for increasing ω/ω_0. For a given k_0d, higher values of d/δ give smoother high frequency behavior and for a given d/δ, lower values of k_0d give smoother high-frequency behavior.

If a non-oscillatory frequency dependence is desired, the parameters k_0d and d/δ will need to be chosen such as to give a non-minimum low-frequency R. In fact, based on the desire to have good high-frequency behavior, the wall thickness should not be much greater than that implied by $k_0d = 0.6$, which is about the maximum radius that one could sacrifice anyway. Figure 5-10 shows how R varies with frequency for $k_0d = 0.6$ and several values of d/δ. The optimum value of d/δ would appear to be in the vicinity of 1.3, i.e., optimum for smooth high-frequency behavior.

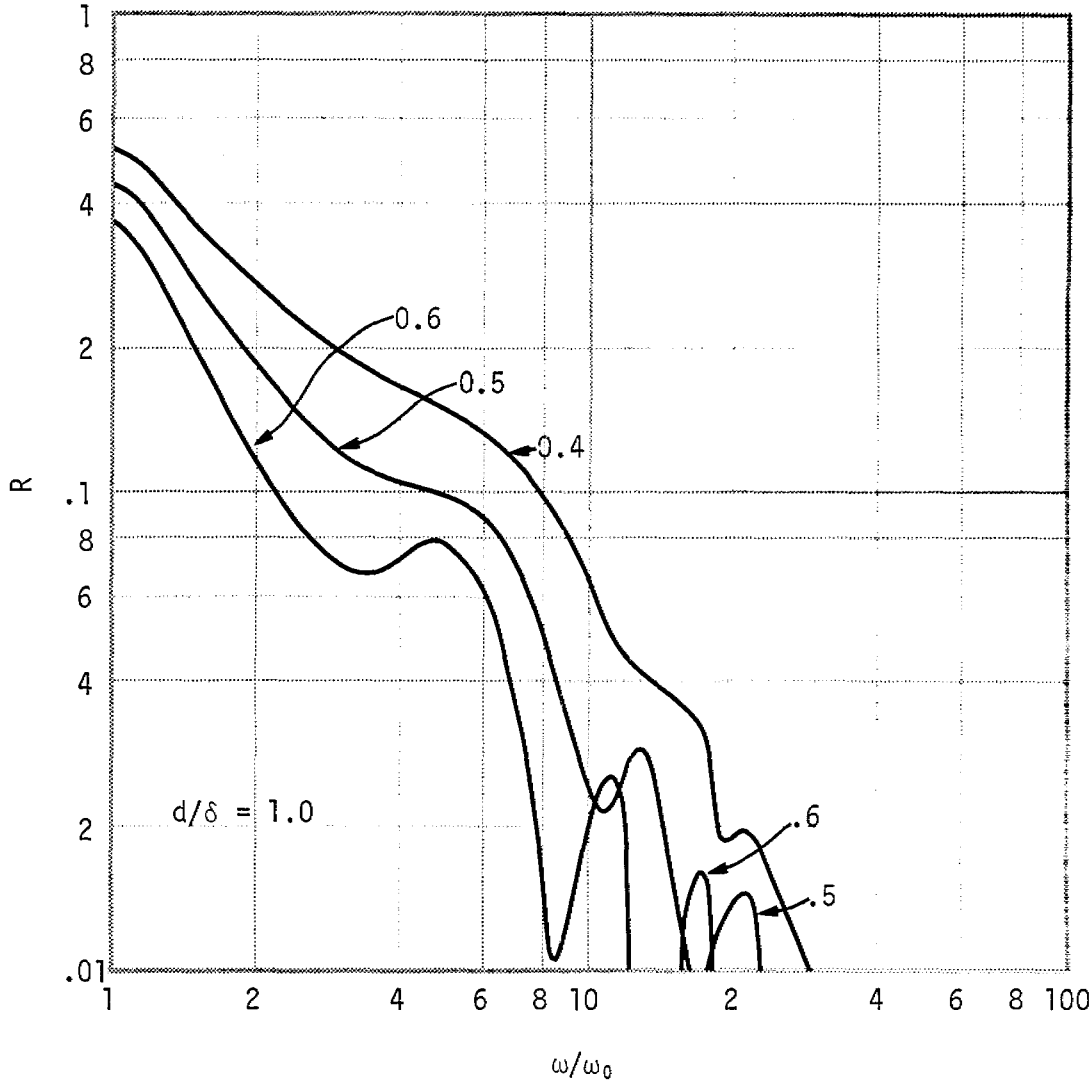

Figure 5-8. Reflection coefficient vs frequency for various $k_0 d$.

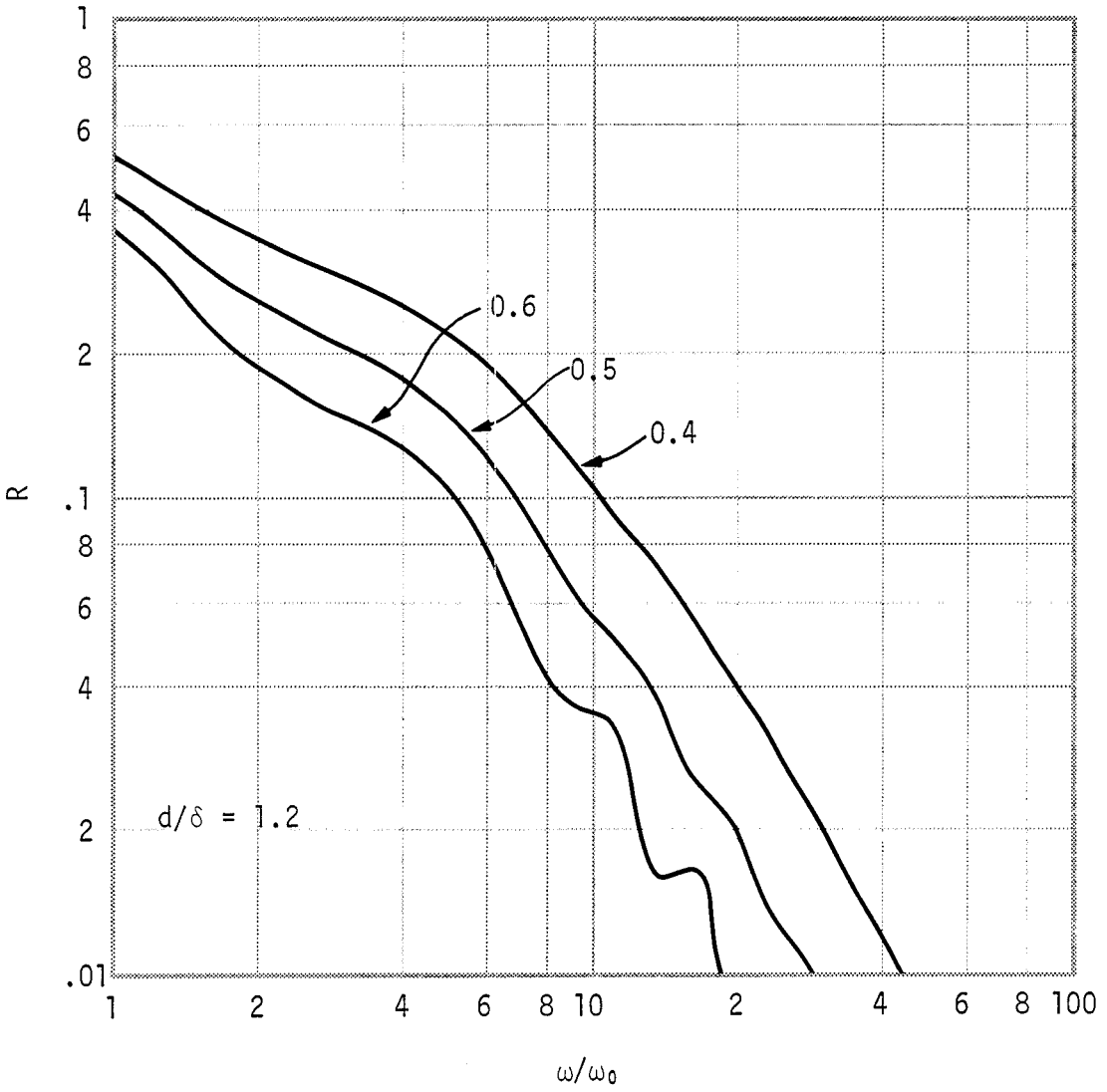

Figure 5-9. Reflection coefficient vs frequency for various $k_0 d$.

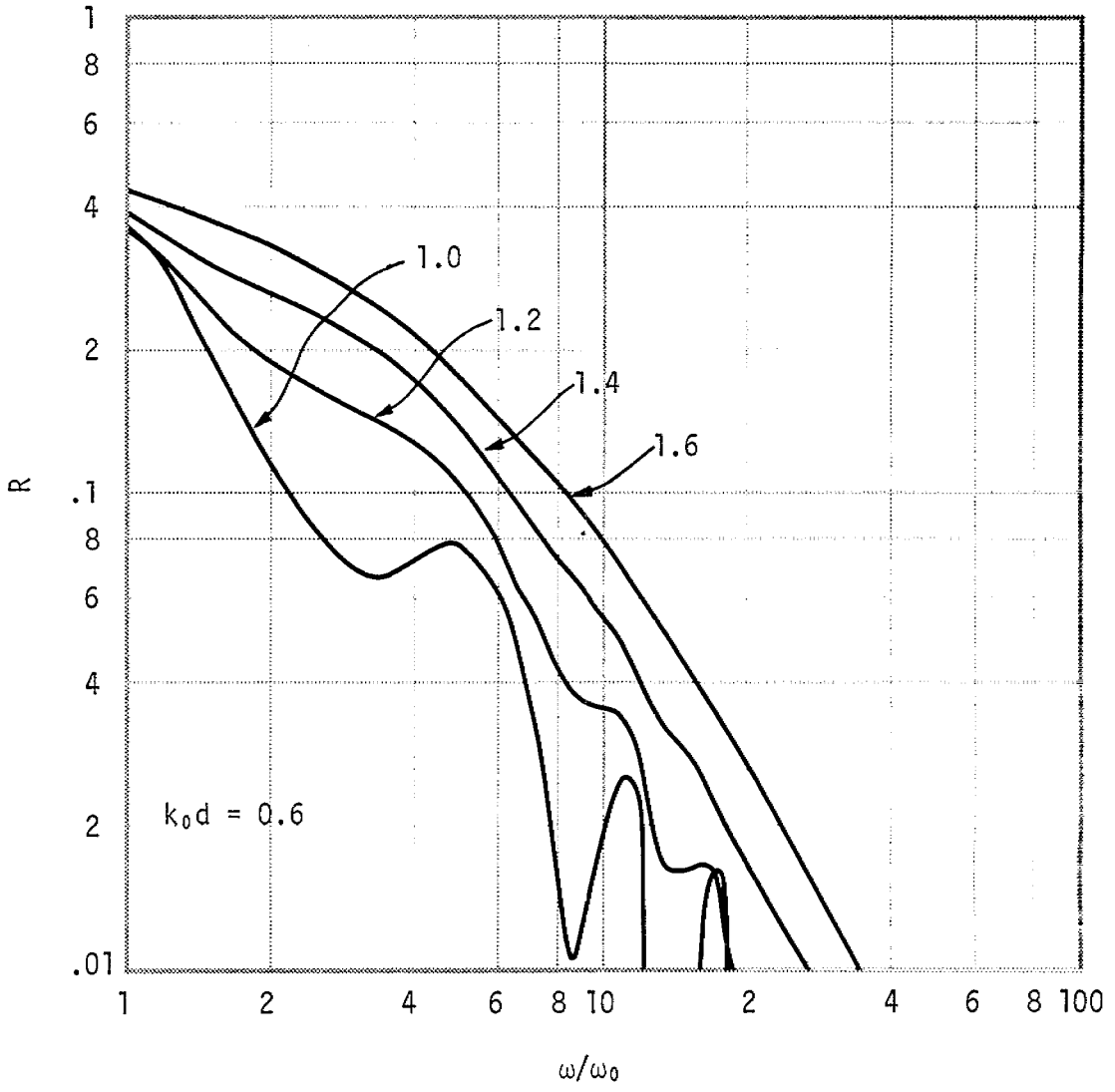

Figure 5-10. Reflection coefficient vs frequency for various d/δ.

Finally, slabs whose conductivities varied with distance were experimented with. Not enough work was performed to draw any real conclusions, but that which was done is interesting. A simple computer code was written which calculates the reflection coefficient for a planer slab with an arbitrary one-dimensional variation in σ and ε. The code was based upon a differential equation for the reflection coefficient derived by Tou (Tou, 1964) for horizontally stratified media. The original intent of the equations was for the calculation of ionospheric reflection coefficients. All that was needed for our purposes was a change in grid size and boundary conditions. Since Tou's paper is probably not generally distributed, the equations will be quickly derived.

Starting with the wave equation,

$$\frac{d^2u}{dx^2} + k_0^2 n^2 u = 0 \tag{5-22}$$

define the incident and reflected waves by

$$u = u_+ + u_- \tag{5-23}$$

where

$$u_+ = Ae^{-ik_0x} \text{(incident wave)} \tag{5-24}$$

$$u_- = Be^{+ik_0x} \text{(reflected wave)} \tag{5-25}$$

A,B = constants

k_0 = free space wave number

n = complex index of refraction.

Differentiating Equation 5-23 with respect to x, obtain

$$u' = - ik_0 u_+ + ik_0 u_- . \tag{5-26}$$

Subtracting

$$ik_0 u = ik_0 u_+ + ik_0 u_- \tag{5-27}$$

from this yields

$$u' - ik_0 u = - 2ik_0 u_+$$

or

$$u_+ = - \frac{u' - ik_0 u}{2ik_0} . \tag{5-28}$$

Adding, instead of subtracting, yields

$$u_- = \frac{u' + ik_0 u}{2ik_0} . \tag{5-29}$$

Define the amplitude reflection coefficient as

$$r = \frac{u_-}{u_+} = - \frac{u' + ik_0 u}{u' - ik_0 u} \tag{5-30}$$

or

$$r = - \frac{u'/u + ik_0}{u'/u - ik_0} . \tag{5-31}$$

Then,

$$\frac{u'}{u} = ik_0 \frac{(r - 1)}{(r + 1)} . \tag{5-32}$$

Differentiating Equation 5-38,

$$\frac{u''}{u} - \left(\frac{u'}{u}\right)^2 = ik_0 \left[\frac{r'}{r + 1} - (r - 1) \frac{r'}{(r + 1)^2} \right]$$

or

$$\frac{u''}{u} - \left(\frac{u'}{u}\right)^2 = ik_0\left[\frac{(r+1)r' - (r-1)r'}{(r+1)^2}\right] . \qquad (5\text{-}33)$$

By the wave equation

$$\frac{u''}{u} = - k_0^2 n^2 .$$

Using this and Equation 5-32

$$\frac{1}{k_0} r' = - \frac{i}{2}\left[(r-1)^2 - n^2(r+1)^2\right] \qquad (5\text{-}34)$$

which is the differential equation for the reflection coefficient. For our calculations, the integration was performed for $y = k_0 x$ instead of x and, since the integration was performed from far distances to close distances, the sign of r was reversed before integrating, leaving the actual equation integrated as

$$\frac{dr}{dy} = \frac{i}{2}\left[(r+1)^2 - n^2(1-r)^2\right] . \qquad (5\text{-}35)$$

The equation is integrated from the perfectly conducting wall where the boundary condition on r is r = 1 (imaginary part is zero) and, by Equation 5-35, $\frac{dr}{dy} = 2i$. The complex arithmetic capability of the CDC 7600 allowed the equation to be differenced directly without rearranging in terms of real and imaginary parts. The energy flow reflection coefficient R was calculated from the amplitude of r. The program was tested by performing constant slab calculations, including an air slab. The errors were entirely negligible.

Before discussing the experiments, we define or review the definition of the following quantities:

1. x: range parameter; x = 0 is the front surface of the slab
2. d: distance to wall

3. y: $k_0 x$

4. e: $k_0 d$

It is important to remember that the calculations were performed for set values of e, not d, and that the curves depicting R vs frequency therefore imply a variation of true slab thickness with frequency. The method used is based upon the idea that we are looking at a single resonant mode and that the change in frequency is due to varying the cavity size. The constant value of e then means that the ratio of slab thickness to chamber radius is held constant. The useful parameter $(\sigma/\varepsilon\omega)$ does not have a meaning with a variable conductivity slab and was simply replaced by ω. The experiments were not well conceived and were performed simply to see if any miraculous gains in damping would jump out at us. If not, the job could probably be done better some other way than a complex tank lining.

In the first experiment, linearly varying conductivities were used. One case was that in which the conductivity rose from 0 at y = 0 to a maximum at the wall. The second case was the inverse, i.e., the conductivity was zero at the wall and maximum at y = 0. The functions were normalized so that their integrals were equal to $\sigma_0 e$, where σ_0 is the conductivity derived from the constant slab problem of equal e. Then, the two linear functions were

$$\sigma_1 = \frac{2\sigma_0}{e} \quad \text{(rising)} \tag{5-36}$$

$$\sigma_2 = \frac{2\sigma_0}{e}(e - y) \quad \text{(falling)} \; . \tag{5-37}$$

Figure 5-11 shows the results for $e = k_0 d = 0.2$. σ_0 was chosen so that the minimum R for the constant slab problem would occur near 30 MHz. In this case, $\sigma_0 = 0.108$ mho/m. The results are inconclusive because all three functions find minima at different frequencies. However, the decreasing function appears to offer a slight improvement while the increasing function appears to make matters worse. One can conclude, however, that the loss mechanism is not purely absorptive, i.e.,

depending only upon the integral of the conductivity.

Figure 5-12 is the same problem with the exception that the maximum conductivity is set equal to σ_0. The resulting R's are about the same as in the first problem, but occur at different frequencies. It is interesting to note that in both problems, the R for the decreasing function was equal to the minimum R for the constant slab at 30 MHz.

The fact that the decreasing functions appear to improve matters, coupled with the success of the membrane method, lead to the final experiment. It was clear that the most effective conducting slabs were those for which the conductivity was concentrated away from the wall. The final calculations were for a constant slab of thickness $\Delta y = k_0 \Delta x$ with the front face at $y = 0$ and with $\sigma \Delta y = \sigma_0 e$. The constants $\sigma_0 = 0.108$ and $e = 0.20$ are the same as in the first two experiments. The ratios $\frac{e}{\Delta y} = \frac{d}{\Delta x}$ used are 1, 2, 4, and 20. Figure 5-13 shows the calculated R's with each curve labeled by its ratio $e/\Delta y$. The minima decrease with increasing $e/\Delta y$, but occur at higher frequencies. The values seen are not much improved, however. It is interesting to compare with the membrane calculations, since the results should converge for large $e/\Delta y$. First calculate the parameter

$$\beta = Z_0 \sigma \Delta x = \frac{Z_0}{k_0} (\sigma \Delta y) \ . \qquad (5\text{-}38)$$

Now $\sigma \Delta y = 0.108(.2) = 2.16 \times 10^{-2}$ mho/m. Then, with $\omega = 2\pi(30 \text{ MHz}) = 1.89 \times 10^8$ rad/sec,

$$\beta = 12.9 \ .$$

The equivalent membrane amplitude reflection coefficient is (Equation 4-17)

$$r = - \frac{\beta}{2 + \beta}$$

so that $r = 0.865$. By Figure 4-3, the R corresponding to this r and $k_0 D = 0.20$ is somewhere around 0.76 to 0.78. This is the same as the

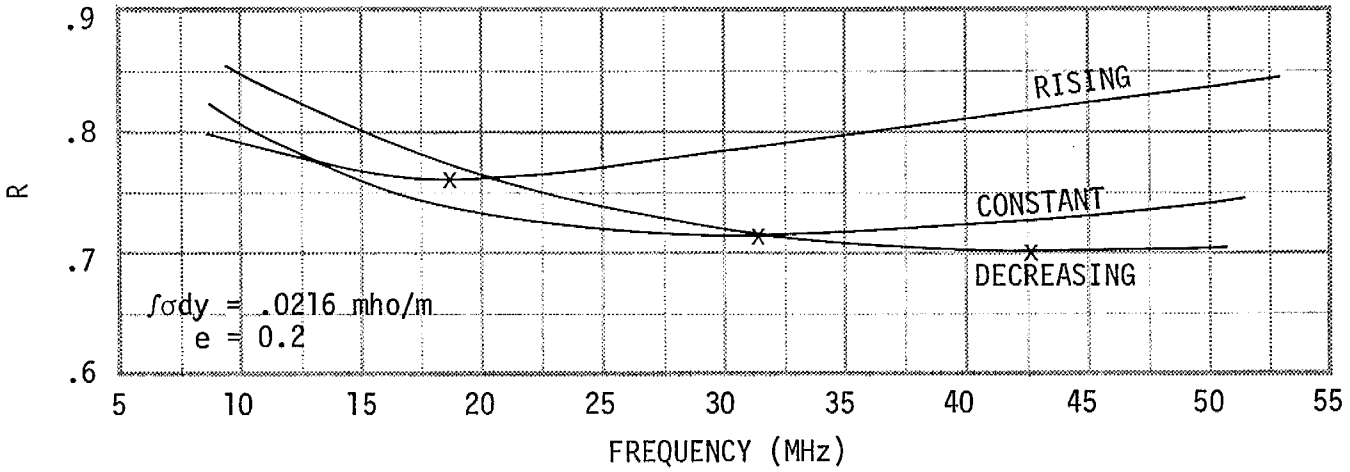

Figure 5-11. Reflection coefficient vs frequency (linear conductivity).

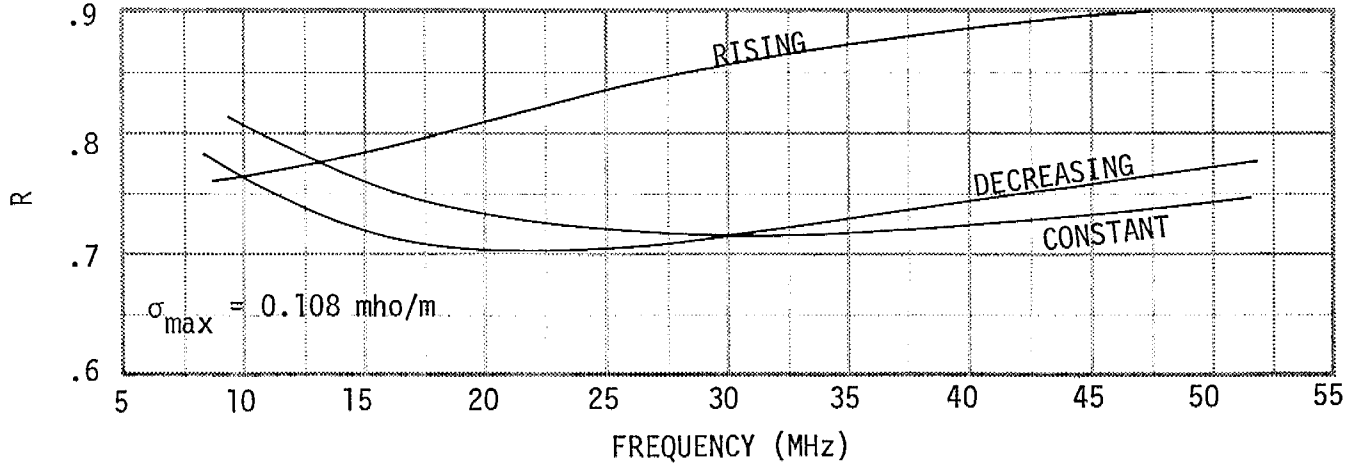

Figure 5-12. Reflection coefficient vs frequency (linear conductivity).

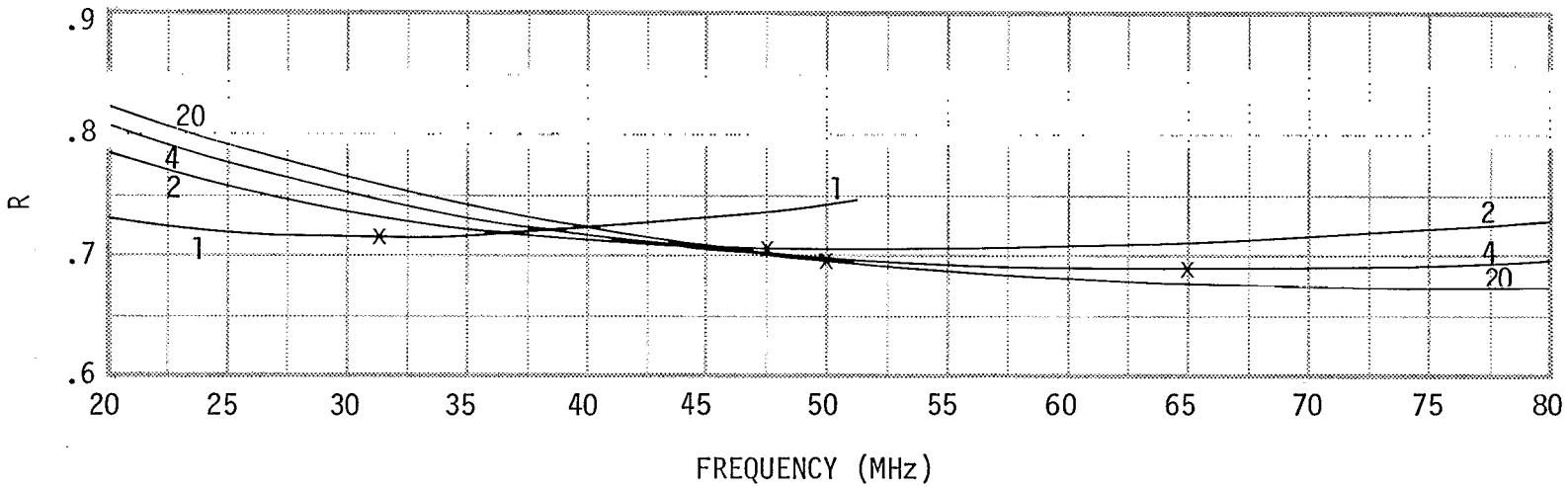

Figure 5-13. Reflection coefficient vs frequency (thin slab) for various ratios of separation distance to thickness.

value of R to which the curves in Figure 5-13 are coverging at 30 MHz.

6. CONCLUSIONS

In this memo, the use of a conducting dielectric layer was investigated for its effectiveness in damping the modal oscillations of the satellite simulator tank. The two basic forms of the layer are (1) a thick conducting dielectric in contact with the wall and (2) a thin membrane some fixed distance from the wall. These are two limiting cases of the general problem and a large investigation of the reflection properties of slabs whose conductivity and permittivity vary with thickness could be made. It is doubtful that significant reductions in energy reflectivity would be attained by using more complex slab models. We note in passing that the tank would not use an actual slab or membrane, but rather an impedance loaded grid which would be modeled after the slab or membrane parameters.

The efficiency of the slabs in absorbing energy is measured by the energy flow reflection coefficient, R. This is related to the Q of a spherical cavity by

$$Q = \frac{k_0(1.45a)}{1 - R} = \frac{3.97}{1 - R} \tag{6-1}$$

(see Section 3) for the fundamental electric mode, where Q is defined by

$$Q \equiv \omega \cdot \frac{\text{(energy in cavity)}}{\text{(energy dissipated/sec)}} . \tag{6-2}$$

Thus, the fraction of contained energy dissipated per cycle is

$$f = \frac{2\pi}{Q} = 1.58\ (1 - R) \tag{6-3}$$

for the fundamental electric mode. These definitions break down for very low values of R. Also, for such low values, the spherical geometry of the real problem must be considered along with the real part of the frequency change.

The investigations presented in this memo indicate that energy reflection coefficients on the order of 0.3 or 0.4 are attainable with both the thin membrane and the thick conducting layer, at a sacrifice of 20 percent of the tank radius. Choosing the R = 0.4 as typical, we see that the tank would have a Q of about 6.5 and that about 95 percent of the energy would be dissipated in one cycle. Even allowing for an error of 10 percent in this figure, one could still expect an energy loss of 85 percent in the first cycle of oscillation for the fundamental electric mode. By Equation 2-45, the real part of the frequency shift would be a reduction by 7 percent of the undamped frequency.

The behavior of the slab and membrane at higher frequencies is of fundamental importance. The membrane has periodic resonances whose spacing depend upon the separation distance between the membrane and the wall. These resonances can be controlled to some extent, but not independently of R. Thus, for certain situations, the reflection properties might be adjusted so that they are acceptable for the frequencies of interest. The thick slab, on the other hand, can be made to have an excellent high-frequency behavior, but, of course, leads to a more complicated grid mock-up. We believe that a grid structure at two or three radii between 0.8a and a could be designed to give adequate damping, without leading to excessive construction problems. Some further calculations are needed, augmented perhaps by some experiments in a mock-up screen room.

REFERENCES

Abramowitz, M., and I. A. Stegun, 1964, Handbook of Mathematical Functions, U. S. Government Printing Office.

Stratton, J. A., 1941, Electromagnetic Theory, McGraw-Ill Book Company.

Tou, C. P., 1964, Scientific Report No. 214, "Techniques for the Determination of Reflection Coefficient and Virtual Height of Low-Frequency Radio Waves," Ionosphere Research Laboratory, Pennsylvania State University.

☆US GOVERNMENT PRINTING OFFICE 1974 — 677-174/18